

# THE EVIDENCE THEORY FOR COLOR SATELLITE IMAGE COMPRESSION

Khaled SAHNOUN and Noureddine BENABADJI

Laboratory of Analysis and Application of Radiation (LAAR)  
Department of Physics, University of Sciences and Technology of Oran  
(USTOMB)  
B.P. 1505, El M'nouar, 31024, ORAN, Algeria

sahnounkhaled@hotmail.fr and benanour2000@yahoo.com

## ABSTRACT

*The color satellite image compression technique by vector quantization can be improved either by acting directly on the step of constructing the dictionary or by acting on the quantization step of the input vectors. In this paper, an improvement of the second step has been proposed. The  $k$ -nearest neighbor algorithm was used on each axis separately. The three classifications, considered as three independent sources of information, are combined in the framework of the evidence theory. The best code vector is then selected, after the image is quantized, Huffman schemes compression is applied for encoding and decoding.*

## KEYWORDS

*Vector quantization, compression,  $k$ -nearest neighbor, Huffman coding, evidence theory.*

## 1. INTRODUCTION

By definition, the compression with vector quantization [1] accepts an input vector  $\vec{x}$  of  $n$  dimension and replaced by a vector  $\vec{y}$  of the same size belonging to a dictionary which is a finite set of code vectors  $(w_j)_{j \in [1, \dots, N]}$  also called classes, or centroids, since they are calculated by an average iterative of vectors  $\vec{x}$ . The quantization step based on the nearest neighbor rule: vector  $\vec{x}$  to classify is assigned to one class of  $(w_j)_{j \in [1, \dots, N]}$  under the condition that this assignment produces the smallest distortion. Such assignment rule may be too drastic in cases where the distances between the vector  $\vec{x}$  and two centroids are very close. A possible improvement to avoid this hard decision would be to consider each color components independently to obtain a classification by component. In this work, components R, G and B are considered as three independent information sources. In a first step, the  $K$ -nearest neighbor rule is applied to all three components, then generating three sets of potential classes. This step, taking into account  $K$ -neighbors and not one, allows considering uncertainty according to each of color components and to push decision making. Finally, the decision of the assignment final class of  $\vec{x}$  is done after combining these three classifications. This technique refers to methods of data fusion. Among all the tools available in this domain, we decide to use the evidence theory [2]

which makes it possible firstly to process uncertain information and secondly to combine information from several sources. In the framework of this theory, several decision rules are defined to enable us selecting the final class of  $\vec{x}$ .

## 2. USE THE EVIDENCE THEORY

### 2.1. Basic principle

Let  $\Omega = \{w_1, \dots, w_N\}$  a set of all possible classes for  $\vec{x}$ , called the frame of discernment and corresponding to the dictionary in our application, the evidence theory extends over the entire power of  $\Omega$ , noted  $2^\Omega$ . We define an initial mass function  $m$  of  $2^\Omega$  in  $[0,1]$  which satisfies the following conditions:

$$\sum_{A \subseteq \Omega} m(A) = 1 \text{ And } m(\emptyset) = 0 \quad (1)$$

Where  $\emptyset$  is the empty set  $m(\emptyset)$ ,  $m(A)$  quantifies the belief that be given to the fact that the class belongs to the subset  $A$  of  $\Omega$ . Subsets  $A$  like  $m(A) > 0$  are called focal elements. Two initial mass functions  $m_1, m_2$  representing the respective information from two different sources, can be combined according to Dempster rule [3]:

$$m(A) = \frac{\sum_{B \cap C = A} m_1(B)m_2(C)}{1 - k} \quad \forall A \in 2^\Omega, A \neq \emptyset \quad (2)$$

$k$  is called the conflict factor and represents the detuning between the two sources, Note that the combination of Dempster also called orthogonal sum and denoted  $m = m_1 \oplus m_2$ .

After combination, a decision on the most likely element of  $\Omega$  must be taken. Several decision rules are possible, but one of the most used is the ‘‘maximum of Pignistic probability’’ Presented by Smets [4] which uses the Pignistic transformation, and allows to evenly distributing the weight associated with a subset of  $\Omega$ , on each of its elements:

$$BandP(\omega) = \sum_{\omega \in A \subseteq \Omega} \frac{m(A)}{|A|}, \forall \omega \in \Omega \quad (3)$$

$|A|$  is the Cardinal of  $A$ . The decision then goes to the element of  $\Omega$ , where the value is the largest.

$$\omega^* = Arg \{max_{\omega \in \Omega} [BandP(\omega)]\} \quad (4)$$

### 2.2. Application to the vector quantization

All compression methods based on the Discrete Cosine Transform (DCT) following three steps, transformation of the difference image or predicted, quantizing and encoding the transformed coefficients [3]. The transformation is applied on blocks of  $8 \times 8$  (pixels) and is defined by:

$$f(u, v) = \frac{2c(u)c(v)}{n} \sum_{x=0}^{n-1} \sum_{y=0}^{n-1} f(x, y) \cos(2x + 1) \frac{u\pi}{2n} \cos(2y + 1) \frac{v\pi}{2n}$$

$$\text{With } c(0) = \frac{1}{\sqrt{2}} \text{ and } c(u) = 1 \text{ if } u \neq 0. \quad (1)$$

$N$  is the block size ( $N = 8$  is selected),  $x, y$  are the coordinates in the spatial domain and  $u, v$  coordinates in the frequency domain. Each block is composed of 64 coefficients. The coefficient

(0.0) is denoted by DC and represents the average intensity of the block, others are denoted AC. The coefficients with the global information of the image are located in low frequency while those in the higher frequencies are often similar to noise [4].

### 2.3. The quantization

We propose to represent the information provided by each independent classification according to each of the three components (R, G, B) by a function of initial mass. These three functions  $(m)_i, i \in \{R, G, B\}$  are created after calculating the K-nearest neighbor and before the final decision they allow to take into account the uncertainty associated with each axis. Thus, classes that are very close to each other on the same axis are grouped in the same focal element, and the decision is made only after having combined the results of the other two projections. For each axis identifies the most significant elements "k" by a distance  $d_i$  on this axis. The initial mass function constructed according to the axis  $i$  has three focal elements  $A_i, \overline{A_i}, \Omega$ .  $\overline{A_i}$  is the complement of  $A_i, i \in \Omega$ . We construct:

$$A_i = \{\omega \in \Omega, \omega = \text{class}(\vec{x}) \mid d_i(\vec{x}, \vec{x}^*) \leq \varepsilon_i(\vec{x}_1, \vec{x}^*), \forall \vec{x}\} \quad (5)$$

$i \in \{R, G, B\}$ .  $\vec{x}^*$  Is the vector for classifying and  $\vec{x}_1$  its nearest neighbor depending on  $d_i$ .  $\varepsilon_i$  is a constant greater than 1 to take into account the sensitivity of the human visual system according to the axis  $i$ , if  $\varepsilon_i = 1$  then  $A_i = \{\text{class}(\vec{x}_1)\}$  is a singleton corresponding to the nearest neighbor. The masses are then assigned to the sets  $A_i$  taking into account the distribution of elements in the set  $A_i$  which is represented by the average distance between two of these elements. The initial mass function for the  $i$  axis then:

$$m_i(A_i) = \alpha_i e^{-\beta_i \overline{d}} \quad (6)$$

$$m_i(\overline{A_i}) = 1 - m_i(A_i) - m_i(\Omega) \quad (7)$$

$$m_i(\Omega) = 0,01 \quad (8)$$

$\alpha_i$  Is a constant and  $\beta_i = 1/d_{max} \cdot d_{max}$  is the maximal distance between  $\vec{x}^*$  and of  $A_i$  elements in (R,G,B) space,  $\overline{d}$  is the average distance between each elements of  $A_i$ . Thus, More  $\overline{d}$  is large more the mass of  $A_i$  is small.  $m_R, m_G, m_B$  The three functions of initial mass from projections R, G and B respectively. Mass function resulting from the combination of three functions is obtained from equation (02):

$$m = m_R \oplus m_G \oplus m_B \quad (9)$$

Finally, assignment class of  $\vec{x}$  is selects from  $m$  equation (09) on the basis of maximum of Pignistic probability equation (03)

## 3. HUFFMAN COMPRESSION FOR R, G AND B

In the proposed compression method, before applying Huffman compression, quantization is applied as it will give better results. In quantization, compression is achieved by compressing a range of values to a single quantum value. When the given number of discrete symbols in a given stream is reduced, the stream becomes more compressible. After the image is quantized, Huffman compression is applied. The Huffman has used a variable-length code table for the encoding of each character of an image where the variable-length code table is derived from the estimated probability of occurrence for each possible value of the source symbol. Huffman has used a

particular method for choosing the representation for each symbol which has resulted in a prefix codes. These prefix codes expresses the most common source symbols using shorter strings of bits than are used for less common source symbols. In this way, we have achieved a compressed image. [5]

#### 4. EXPERIMENTAL RESULTS AND DISCUSSION

Four different color images have been taken for experimental purpose. Simulation results for different images are given in Table 1. For measuring the originality of the compressed image Peak Signal to Noise Ratio (PSNR) is used, which is calculated using the formula

$$PSNR(db) = 10 \log_{10} 255^2 / MSE \quad (10)$$

Where MSE is the mean squared error between the original image  $f_{ij}$  and the reconstructed compressed image  $f'_{ij}$  of the size MN, which is calculated by the equation[6]

$$MSE = \frac{1}{MN} \sum_{j=1}^M \sum_{i=1}^N [(f'_{ij}) - (f_{ij})]^2 \quad (11)$$

The algorithm realized in Builder C++ to code and to decode the satellite image, but all these Images are resized into a resolution of 256 X 256.



Figure 1. Original Satellite image (1)

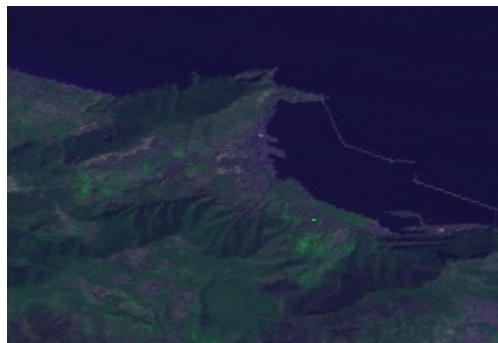


Figure 2. Reconstructed Satellite image (1)



Figure 3. Original image 'Lena'



Figure 4. Reconstructed image 'Lena'



Figure 5. Original Satellite image (2)



Figure 6. Reconstructed Satellite image (2)

<b>Image</b>	<b>PSNR(db)</b>	<b>CR</b>
<b>Lena</b>	32.92	13.66
<b>Satellite image (1)</b>	34.68	15.89
<b>Satellite image (2)</b>	33.89	15.55

Table 1. The compression ratios and PSNR values derived for imageries

It can be seen from the Table 1 that for all the images, the PSNR values are greater than 32, the compression ratios achievable different. It is clearly evident from the table that for two types of images with reasonably good PSNR values clearly indicate that the compression ratio achievable for satellite imageries is much higher compared to the standard Lena image.

## 5. CONCLUSIONS

To improve the quantization step of the input vectors according to the code vectors present in a dictionary. Using the evidence theory has obtaining promising results. In our study setting, a vector quantization was performed on each of the three colors R, G and B, according to the color dispersion of the K-nearest neighbor. The results show that the use of evidence theory during the quantization step and Huffman coding is an improvement of the quality of the reconstructed images

## REFERENCES

- [1] A. Gersho and R. M. Gray. Vector Quantization and Signal Compression. Kluwer Academic Publishers, 1991.
- [2] G. Shafer. A mathematical theory of evidence. Princeton University Press, 1976.
- [3] A. Dempster. Upper and Lower Probabilities Induced by Multivalued Mapping. Ann. Math. Statist , 38:325– 339, 1967.
- [4] P. Smets. Constructing the pignistic probability function in a context of uncertainty. Uncertainty in Artificial Intelligence, 5 :29–39, 1990. Elsevier Science Publishers.
- [5] H.B.Kekre, Tanuja K Sarode, Sanjay R Sange “ Image reconstruction using Fast Inverse Halftone & Huffman coding Technique”, IJCA, volume 27-No 6, pp.34-40, 2011
- [6] Varun Setia, Vinod Kumar, “Coding of DWT Coefficients using Run-length coding and Huffman Coding for the purpose of Color Image Compression”, IJCA, volume 27-No 6, pp.696-699, 2012.